Monotone embedded discrete fractures method for flows in porous media: experiments

Kirill D. Nikitin * Ruslan M. Yanbarisov

March 5, 2019

1 Numerical experiments

In this section we consider four numerical experiments:

- The first two experiments are designed to study the ability of the mEDFM to preserve solution non-negativity or to satisfy the discrete maximum principle (DMP) for different discretization schemes for (**??**). We consider two benchmark problems [1] to which several highly permeable fractures are added to the domain.
- The third experiment is a standard single-phase flow benchmark test "Hydrocoin" [2]. This test verifies the mEDFM by comparing with the fine grid solution.
- The fourth experiment is unsteady two-phase flow model test with several wells and fractures. The mEDFM is compared with the discrete fracture method (DFM) based on mesh modification.

1.1 Test for solution non-negativity

The experiment setup is the following. The computational domain is $\Omega = \Omega_1 \setminus \Omega_2,\ \Omega_1 = [0,1]^3, \Omega_2 = [0.4, 0.6]^3$. We solve the diffusion equation with Dirichlet boundary conditions (see Figure 1):

*Marchuk Institute of Numerical Mathematics, Russian Academy of Sciences, Moscow; nikitin.kira@gmail.com

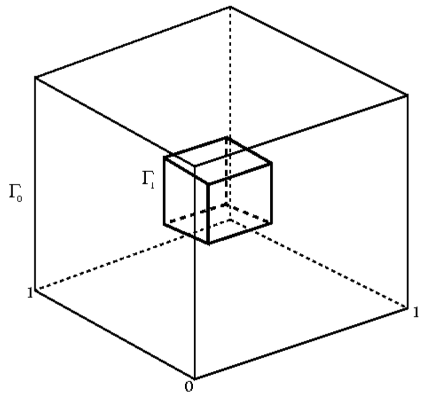

$$
\begin{aligned}
-\mathrm{div}\, \mathbb{K}\nabla p &= 0,\\
p|_{\Gamma_0} &= 0,\\
p|_{\Gamma_1} &= 2.
\end{aligned}
\tag{1}
$$

$$
\mathbb{K} = R_{xyz} \begin{pmatrix} 300 & 0 & 0 \\ 0 & 15 & 0 \\ 0 & 0 & 1 \end{pmatrix} R_{xyz}^T,
$$

$$
R_{xyz} = R_z(-\pi/6) R_y(-\pi/4) R_x(-\pi/3).
$$

Figure 1: Non-negativity test set-up.

The differential solution for this problem is from 0 to 2, and Theorem **??** states that the discrete solution must be non-negative if the monotone NTPFA is used in mEDFM.

We modify the proposed test by inserting two rectangular fractures and solve (1) on $20 \times 20 \times 20$ cubic mesh (see Figure 2). The first fracture is a vertical rectangle with corner points $A_1 = (0.27, 0.11, 0.11)$, $B_1 = (0.77, 0.31, 0.51)$, the second one is a vertical rectangle with corner points $A_2 = (0.26, 0.51, 0.71)$, $B_2 = (0.76, 0.91, 0.66)$. Fractures widths are $w_{f,1} = w_{f,2} = 0.01$, fracture permeabilities are isotropic: $\mathbb{K}_{f,1} = 5000\,\mathbb{I}, \mathbb{K}_{f,2} = 50000\,\mathbb{I}$.

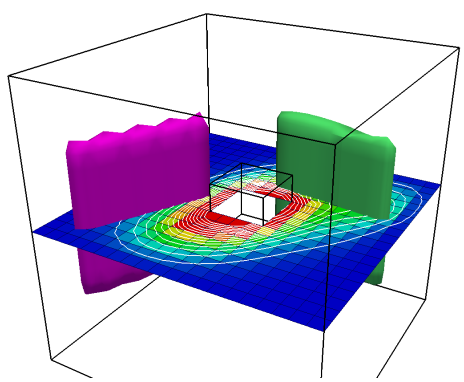

Figure 2: Non-negativity test: fractures location.

Table 1 shows minima and maxima of the FV solution by TPFA, NTPFA (non-negative) and MPFA-O schemes in the domain without fractures and with two fractures. In the latter case, mEDFM is applied to account the fractures. Both TPFA and NTPFA preserve non-negativity of the FV solution for the test without fractures and the test with fractures, while the linear MPFA-O scheme violates non-negativity in both cases. It is important that MPFA-O FV discretization of (**??**) produces negative solutions even inside fractures despite the fact that the discretization scheme for (**??**) is non-negativity preserving linear TPFA. Using the linear TPFA FV discretization for (**??**) provides solution non-negativity but has no approximation, see Figures 3, 4.

	$min(p)$	$max(p)$	$min(p_f)$	$max(p_f)$
domain without fractures				
TPFA	9.8e-5	1.7546	-	-
NTPFA	1.6e-7	1.9177	-	-
MPFA-O	-0.2196	2.0692	-	-
domain with two fractures				
mEDFM (TPFA)	9.5e-5	1.7542	0.1861	0.4624
mEDFM (NTPFA)	1.6e-7	1.9166	0.1398	0.6261
mEDFM (MPFA-O)	-0.1758	2.0620	-0.0094	0.5949

Table 1: Minima and maxima of the FV solutions in porous media and fractures for the non-negativity test.

Figures 3 and 4 illustrate the FV solutions on the mesh cross-section for the three schemes in the domain without fractures and with them, respectively. The noisy isolines for the MPFA-O scheme indicate the negative solution areas.

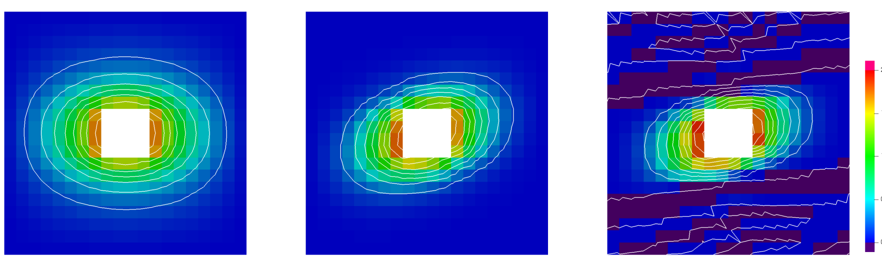

TPFA NTPFA MPFA-O

Figure 3: Non-negativity test: FV solution for the domain without fractures (undershoots are colored in dark blue).

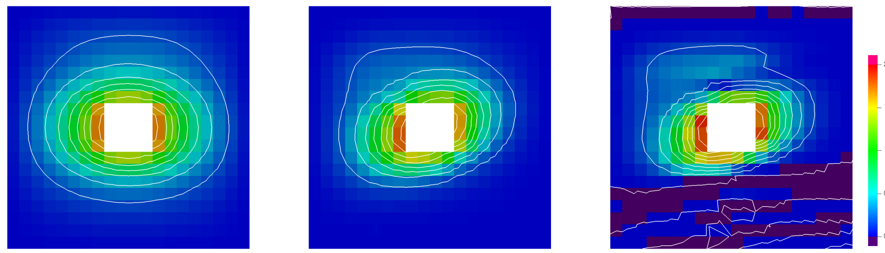

mEDFM (TPFA) mEDFM (NTPFA) mEDFM (MPFA-O)

Figure 4: Non-negativity test: FV solution for the domain with two fractures (undershoots are colored in dark blue).

1.2 Test for the discrete maximum principle

The second test studies the discrete maximum principle (DMP) property of the discretization schemes. The domain is the unit cube without two boxes imitating wells: $\Omega = [0,1]^3 \setminus (\Omega_1 \cup \Omega_2)$, $\Omega_1 = [3/11, 4/11] \times [5/11, 6/11] \times (0,1)$, $\Omega_2 = [7/11, 8/11] \times [5/11, 6/11] \times (0,1)$.

$p = 0 \text{ on } \Gamma_0, \quad p = 1 \text{ on } \Gamma_1, \quad \mathbb{K}\nabla p \cdot \mathbf{n} = 0 \text{ on } \Gamma_{\text{out}}$

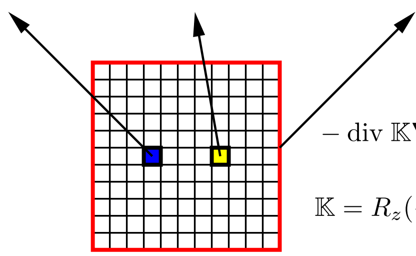

$$-\operatorname{div} \mathbb{K}\nabla p = 0,$$

$$\mathbb{K} = R_z(-67.5^\circ) \begin{pmatrix} 1 & 0 & 0 \\ 0 & 10^{-3} & 0 \\ 0 & 0 & 1 \end{pmatrix} R_z(67.5^\circ).$$

Figure 5: DMP test setup.

By analogy with the first test, we consider two problem settings. The first setting corresponds to the domain without fractures (Figure 5). The second setting has 3 vertical rectangular fractures with the following corner points (Figure 6):

$A_1 = (0.16, 0.326795, 0), \quad B_1 = (0.36, 0.673205, 1),$

$A_2 = (0.41, 0.326795, 0), \quad B_2 = (0.61, 0.673205, 1),$

$A_3 = (0.66, 0.326795, 0), \quad B_3 = (0.86, 0.673205, 1).$

Fractures locations are chosen to test possible DMP violations. Fractures width is $w_{f,i} = 0.01$ and permeability in fractures is isotropic, $\mathbb{K}_{f,i} = \mathbb{K}_f = 1000\mathbb{I}$, $i = 1, 2, 3$.

Table 2 shows minima and maxima of the FV solution by TPFA, MPFA-O, NTPFA (non-negative) and NMPFA (satisfying DMP) schemes in the domain without fractures and with three fractures. In the latter case, mEDFM is applied to account for the fractures. The mEDFM with linear TPFA, as expected, provides no approximation but preserves maximum and minimum of the discrete solution. Both MPFA-O and NTPFA discretizations violate the DMP, while MPFA-O discretization also violates solution non-negativity. Similar to the previous test case, the schemes violating the DMP, generate undershoots and overshoots even in fractures, despite the fact that the discretization scheme for (**??**) is linear TPFA satisfying the DMP. Only the NMPFA scheme with the DMP preserves both maximum and minimum while showing reasonable solution. Figure 1.3 presents the FV solutions of the problem on a mesh cross-section.

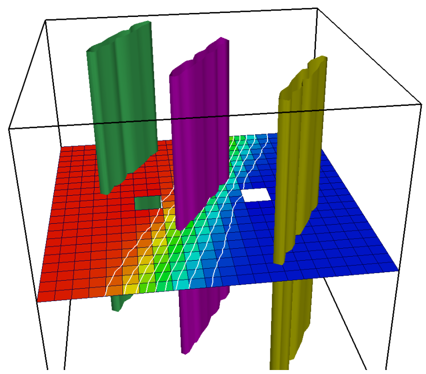

Figure 6: DMP test: fractures location.

	$min(p)$	$max(p)$	$min(p_f)$	$max(p_f)$
domain without fractures				
TPFA	0.0244	0.9756	-	-
NTPFA	0.0061	1.8898	-	-
NMPFA	0.0072	0.9928	-	-
MPFA-O	-0.0261	1.0261	-	-
domain with three fractures				
mEDFM (TPFA)	0.0245	0.9755	0.1376	0.8534
mEDFM (NTPFA)	0.0063	1.7395	0.1131	1.3636
mEDFM (NMPFA)	0.0074	0.9925	0.0244	0.9750
mEDFM (MPFA-O)	-0.0459	1.0442	-0.0015	0.9995

Table 2: Minima and maxima of the FV solution in porous media and fractures for the DMP test.

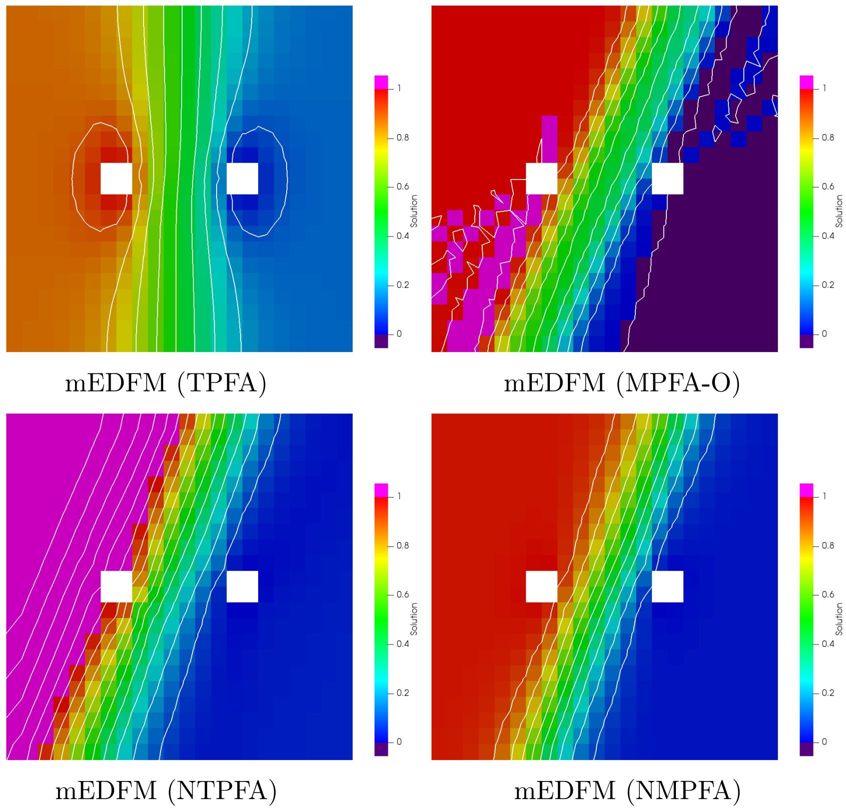

Figure 7: DMP test: FV solutions for the domain with three fractures (overshoots and undershoots are colored in pink and dark blue respectively).

1.3 Hydrocoin test

A single-phase flow benchmark was proposed in the international Hydrocoin project for heterogeneous groundwater flow problems. The 2D domain in a vertical plane contains two intersecting fractures, see Figure 8. The pressure (hydraulic head) is prescribed on the top boundary and Neumann no-flow on the other three boundaries. Figure 9 presents the non-orthogonal computational grid used in this test. The permeabilities (hydraulic conductivities) are 10^{-6} m / s in the fractures and 10^{-8} m / s in the rock matrix.

Figure 10 shows the mEDFM (NTPFA) solution on 32×23 mesh. Figure 11 demonstrates comparison of three solutions along the line $z = -200$: the mEDFM (NTPFA) solution on coarse 32×23 mesh (blue), the EDFM solution [2] (red) and the reference fine grid solution with fractures represented by cells (black). One can observe good agreement of the mEDFM solution to the reference.

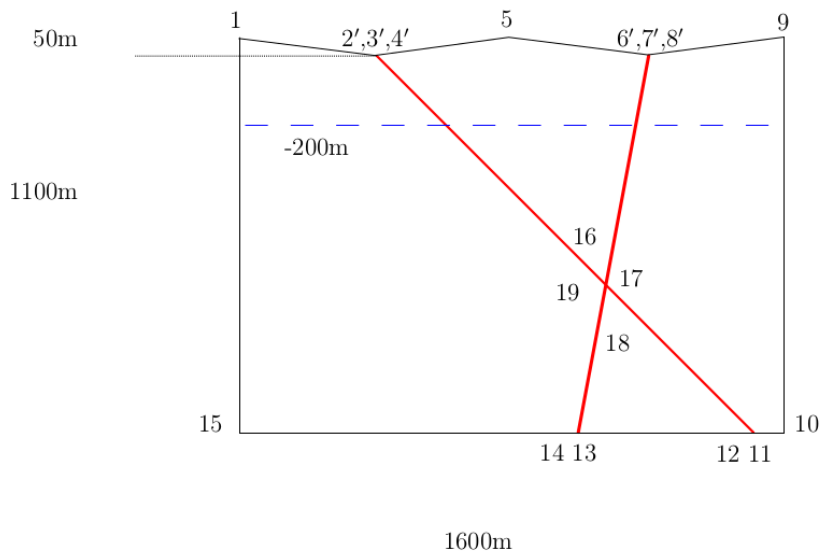

Figure 8: Domain and fractures for the Hydrocoin test. The solution should be verified at the dashed line.

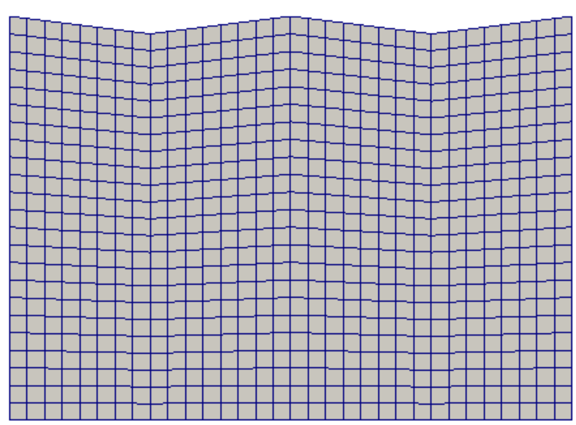

Figure 9: Computational grid for the Hydrocoin test.

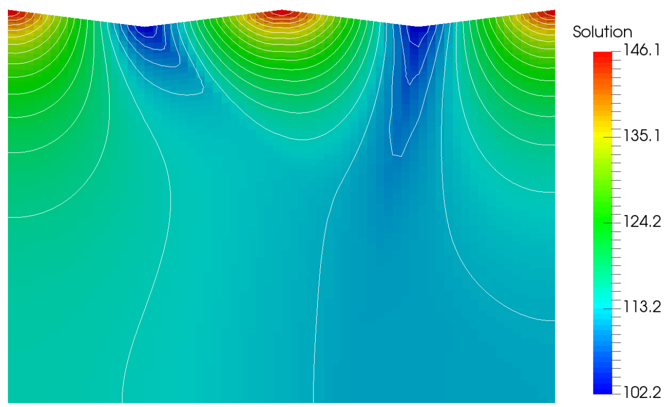

Figure 10: mEDFM+NTPFA solution of the Hydrocoin test.

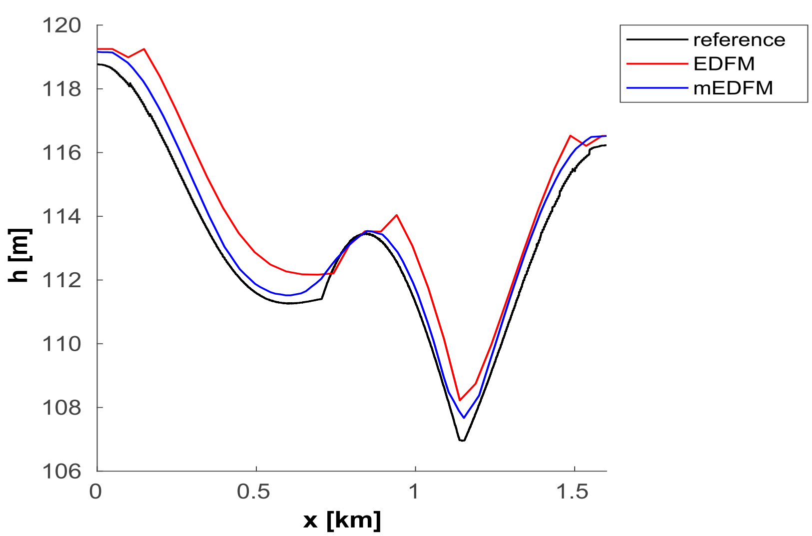

Figure 11: Comparison of the FV solutions traces on the level -200 m: fine grid reference solution (black), EDFM solution [2] (red), mEDFM (NTPFA) solution on the coarse mesh with 32x23 cells(blue).

1.4 Verification of mEDFM through DFM for two-phase flow

In the last test we simulate a two-phase flow with one injecting well, one producing well and a fracture close to the injector. The experiment setup is shown in Figure 12. For the wells we set the bottom hole pressures $p_{inj} = 4100psi$ and $p_{prod} = 3900psi$.

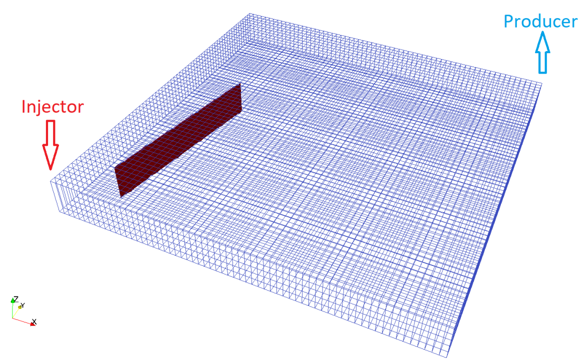

Figure 12: Five-spot problem with fracture setup.

The matrix permeability tensor is $\mathbb{K} = diag(100, 100, 1)$ and matrix porosity is $\phi = 0.15$. The fracture permeability tensor is $\mathbb{K}^f = diag(10000, 10000, 1)$ and fracture porosity is $\phi^f = 0.85$. Tables for capillary pressure dependencies are similar to two-phase flow experiments from [3]. We use the simple TPFA discretization for (**??**) and (**??**) since the mesh is $\mathbb{K}$-orthogonal.

We simulate water injection for 50 days with time step $\Delta t = 1$ day and compare the mEDFM (TPFA) solution with the DFM-FV (NTPFA) solution obtained on the mesh with cut-cells and direct representation of fractures. Figure 13 shows the oil pressure field at different times of the simulation. Figure 14 presents the water saturation field. One can see very close agreement of the solutions obtained by different methods.

a)

b)

c)

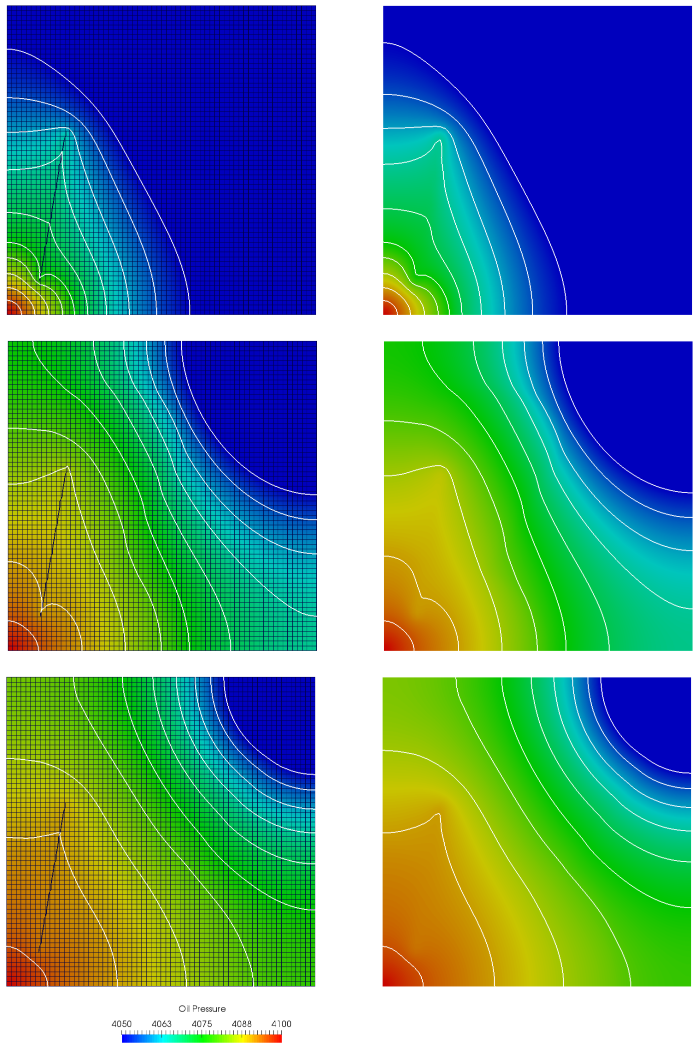

Figure 13: Oil pressure field for the two-phase flow: a) T = 2, b) T = 21, c) T = 50 days. Left: DFM-FV (NTPFA) solution; right: mEDFM-TPFA solution.

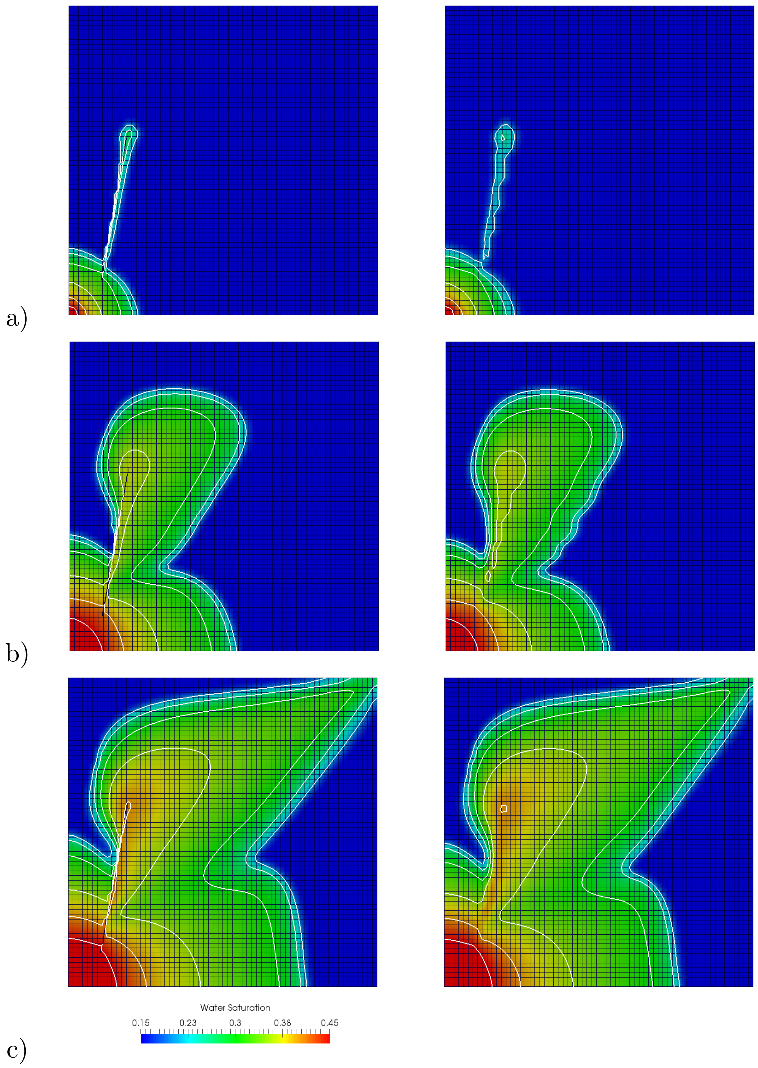

Figure 14: Water saturation field for two-phase flow: a) T = 2, b) T = 21, c) T = 50 days. Left: DFM-FV solution; right: mEDFM-TPFA solution.

References

[1] A. A. Danilov and Y. V. Vassilevski. A monotone nonlinear finite volume method for diffusion equations on conformal polyhedral meshes. *Russ. J. Numer. Anal. Math. Model.*, 24(3):207–227, 2009.

[2] B. Flemisch, I. Berre, W. Boon, A. Fumagalli, N. Schwenck, A. Scotti, I. Stefansson, and A. Tatomir. Benchmarks for single-phase flow in fractured porous media. *Adv. Water Resour.*, 111:239–258, 2018.

[3] K. Nikitin, K. Terekhov, and Y. Vassilevski. A monotone nonlinear finite volume method for diffusion equations and multiphase flows. *Comput. Geosci.*, 18(3):311–324, 2014.